

A Rearrangement Reaction to Yield a NH_4^+ Ion Driven by Polyoxometalate Formation

N. Tanmaya Kumar, Shivaiah Vaddypally, and Samar K. Das*

Cite This: *ACS Omega* 2022, 7, 31474–31481

Read Online

ACCESS |



Metrics & More

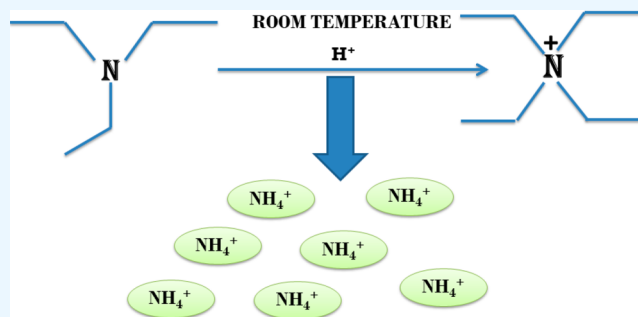


Article Recommendations



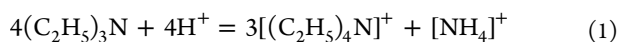
Supporting Information

ABSTRACT: Triethylamine is a volatile liquid and exists in the atmosphere in the gas phase. It is a hazardous air pollutant and identified as a toxic air contaminant. Thus, producing ammonia (a vital chemical for fertilizer production) from the vapor state of this toxic substance is a challenging task. Diffusion of the vapor of triethylamine, $(\text{C}_2\text{H}_5)_3\text{N}$, into an acidified aqueous solution of sodium molybdate results in the formation of single crystals of compound **1** $[(\text{C}_2\text{H}_5)_3\text{NH}]_2[(\text{C}_2\text{H}_5)_4\text{N}][\text{NaMo}_8\text{O}_{26}]$ (**1**). Notably, compound **1** includes a $[(\text{C}_2\text{H}_5)_4\text{N}]^+$ cation, even though the concerned reaction mixture was not treated with any tetraethylammonium salt. The formation of the $[(\text{C}_2\text{H}_5)_4\text{N}]^+$ cation from $(\text{C}_2\text{H}_5)_3\text{N}$ in an acidic aqueous medium is logically possible only when an ammonium cation (NH_4^+) is formed in the overall reaction: $4(\text{C}_2\text{H}_5)_3\text{N} + 4\text{H}^+ = 3[(\text{C}_2\text{H}_5)_4\text{N}]^+ + [\text{NH}_4]^+$. Although the resulting NH_4^+ cation (identified by Nessler's reagent test) is not included in the crystals of compound **1** as a cation, it can be made associated with a crown ether in the isolation of single crystals of compound $[\text{NH}_4\text{C}15\text{C}5]_3[\text{PMo}_{12}\text{O}_{40}]\cdot\text{B}15\text{C}5$ (**2**), (B15C5 = benzo-15-crown-5). Crystal structure analysis and ^1H NMR studies of compound **2** have established the presence of an H-bonded NH_4^+ ion in compound **2**, thereby established the rearrangement reaction.



INTRODUCTION

Ammonia is an essential inorganic chemical for the fertilizer industry, is the sixth largest chemical produced in the world,^{1–4} and is the key precursor of synthetic fertilizer.^{5–7} Until recently, Haber's process was the frequently used method for industrial production of ammonia, which involves molecular nitrogen and hydrogen and requires drastic conditions (500 °C at 150–200 atm).^{8–10} In nature, nitrogenase enzymes containing iron and molybdenum cofactors (known as FeMoCo) do the job of production of ammonia from atmospheric nitrogen at ambient conditions.^{11–13} There are various reports where ammonia is generated using transition-metal catalyzed reduction of nitrogen gas,^{14–24} as well as through electrochemical^{25–33} and photo(electro)chemical methods.^{34–38} We have demonstrated here a unique inorganic rearrangement (not a redox reaction), occurring at room temperature, that involves diffusion of triethylamine vapor into an acidic aqueous polyoxomolybdate solution to generate an ammonium ion (NH_4^+) and tetraethylammonium ion ($[(\text{C}_2\text{H}_5)_4\text{N}]^+$) as shown in eq 1, resulting in the isolation of single crystals of compound $[(\text{C}_2\text{H}_5)_3\text{NH}]_2[(\text{C}_2\text{H}_5)_4\text{N}][\text{NaMo}_8\text{O}_{26}]$ (**1**). Notably, compound **1** includes the resulting tetraethylammonium cation ($[(\text{C}_2\text{H}_5)_4\text{N}]^+$) but not the ammonium cation (NH_4^+).



There are quite a few inorganic rearrangement reactions reported. The Michaelis–Arbuzov rearrangement for the formation of C–P bonds,³⁹ intermolecular rearrangements in boron clusters,⁴⁰ and rearrangement of polyamines⁴¹ are a few of them. These rearrangement reactions have found numerous applications in various fields. The rearrangement, described here, will be an addition to this family of inorganic rearrangement reactions as it demonstrates the rearrangement of triethylamine to a tetraethylammonium ion and most importantly ammonium ions at room temperature.

Triethylamine is a colorless liquid (boiling point, 89.5 °C), but it exists in the atmosphere in the gas phase. According to the United States Environmental Protection Agency (U.S. EPA), the concentration of triethylamine in ambient air was as high as 4.2 μg per cubic meter or 1 part per billion from an unspecified location in the northeast United States in 1983.⁴² Thus, use of triethylamine in its vapor state to generate ammonia would be a challenging task. In the present work, we have demonstrated the formation of an ammonium ion from

Received: June 27, 2022

Accepted: August 11, 2022

Published: August 23, 2022



triethylamine vapor (eq 1) at room temperature; the work was initiated from a serendipitous observation (*vide infra*). Even though the resulting ammonium ion is not included in the crystals of compound $[(C_2H_5)_3NH]_2[(C_2H_5)_4N][NaMo_8O_{26}]$ (1), we could succeed to manipulate the ammonium ion (NH_4^+), formed in the rearrangement (eq 1), to be associated with a crown-ether (benzo-15-crown-5, B15C5) in forming a ammonium-crown-ether supramolecular cation, which has been crystallized with a Keggin type polyoxometalate anion ($[PMo_{12}O_{40}]^{3-}$) resulting in the single crystals of compound $[NH_4^+C(B15C5)_3][PMo_{12}O_{40}] \cdot B15C5$ (2). We have characterized compounds 1 and 2 by routine spectral analyses, including elemental analyses, and unambiguously by single crystal X-ray crystallography. We have established the rearrangement reaction (eq 1), which is the formation of $[(C_2H_5)_4N]^+$ and $[NH_4]^+$ cations from $(C_2H_5)_3N$, by single crystal X-ray structure determination of compounds 1 and 2, and also we have identified the resulting ammonium ion (NH_4^+), formed in the rearrangement reaction (eq 1), by Nessler's reagent test, IR, and ESI-mass spectroscopies, and TGA studies.

EXPERIMENTAL SECTION

Materials and Methods. All the starting materials were purchased as analytical grade and were used as received. IR spectra of the compounds were obtained on a JASCO-5300 FTIR spectrophotometer. TGA was carried out on an STA 409 PC analyzer. PXRD plots were recorded on a Bruker D8-Advance diffractometer using graphite-monochromated $Cu K\alpha_1$ (1.5406 Å) and $K\alpha_2$ (1.55439 Å) radiation. NMR spectra were recorded on a Bruker Advance-500 MHz FT NMR spectrometer using tetramethylsilane (TMS, $\delta = 0$) as the internal standard and DMSO- d_6 as the solvent, at room temperature. The mass spectral studies were carried out on a Bruker Maxis HRMS instrument using ESI techniques.

Synthesis of $[(C_2H_5)_3NH]_2[(C_2H_5)_4N][NaMo_8O_{26}]$ (1). Sodium molybdate (3.5 g, 14.46 mmol) was dissolved in 50 mL of water followed by the addition of 10 mL of glacial acetic acid (100%) with stirring at room temperature. This reaction mixture was then acidified to pH 2 by the dropwise addition of concentrated HNO_3 , which resulted in an almost clear solution. The resultant mixture was filtered into a 100 mL beaker. This 100 mL beaker was then kept in a 250 mL beaker containing triethylamine liquid, and the 250 mL beaker was covered with aluminum foil. The setup was then kept at room temperature for 3 days. The crystals of compound 1, precipitated during this time, were filtered, washed with cold distilled water, and dried at room temperature. Yield: 1.6 g (59% based on Mo). Anal. Calcd (in %) for $C_{20}H_{52}Mo_8N_3NaO_{26}$: C, 15.59; H, 3.40; N, 2.73. Found: C, 14.08; H, 2.95; N, 2.10.

Synthesis of $[NH_4^+C(B15C5)_3][PMo_{12}O_{40}] \cdot B15C5$ (2). To a stirred solution of benzo-15-crown-5 (0.03 g, 0.13 mmol) in 50 mL of acetonitrile was added $H_3[PMo_{12}O_{40}] \cdot xH_2O$ (0.16g, 0.09 mmol). After all reactants were dissolved, 20 mL of the filtrate of the compound 1 crystals was added, followed by 10 mL of glacial acetic acid (100%). The resulting solution was stirred at room temperature for 18 h, filtered, and allowed to evaporate slowly. Brown crystals of compound 2 were obtained after 1 week. These were filtered from the mother liquor thereafter and dried at room temperature. Yield: 0.108 g (67.5% based on Mo). Anal. Calcd (in %) for $C_{56}H_{92}Mo_{12}N_3O_{60}P$: C, 22.80; H, 3.14; N, 1.42. Found C, 23.05; H, 3.18; N, 1.36.

Crystal Data Collection. X-ray reflections were collected on a Bruker D8 QUEST CCD diffractometer equipped with a graphite monochromator and a Mo $K\alpha$ fine-focus sealed tube ($\lambda = 0.71073$ Å), and the reduction was performed using APEX-II Software.⁴³ Intensities were corrected for absorption using SADABS, and the structure was solved and refined using SHELX-97.⁴⁴ All non-hydrogen atoms were refined anisotropically. Hydrogen atoms on non-hydrogen atoms were located from difference electron-density maps, and all C–H atoms were fixed geometrically. Hydrogen-bond geometries were determined in PLATON.^{45,46} Crystal parameters are shown in Table 1. Bond lengths and bond angles of compounds 1 and 2

Table 1. Crystal Parameters of Compounds 1 and 2

compound	1	2
formula	$C_{20}H_{52}Mo_8N_3NaO_{26}$	$C_{56}H_{92}Mo_{12}N_3O_{60}P$
formula weight	1541.14	2949.56
temperature (K)	296	273(2)
wavelength (Å)	0.71073	0.71073
crystal system, space group	monoclinic, $C2/c$	triclinic, $P\bar{1}$
<i>a</i> (Å)	24.9768(13)	13.6148(15)
<i>b</i> (Å)	11.1607(5)	14.8087(17)
<i>c</i> (Å)	18.0093(9)	25.588(3)
α (deg)	90	100.368(2)
β (deg)	120.271(2)	97.571(2)
γ (deg)	90	111.955(2)
volume (Å ³)	4335.7(4)	4593.3(9)
<i>Z</i> , ρ (g/cm ³)	4, 2.358	1, 2.159
μ (mm ⁻¹)	2.332	1.707
<i>F</i> (000)	3900.0	2920.0
goodness-of-fit on <i>F</i> ²	1.178	1.046
R1	0.0364	0.0755
wR2	0.1046	0.2033
largest diff. peak/hole (e Å ⁻³)	3.65	7.29

are summarized in Table S2 and Table S3, respectively (Supporting Information). Crystallographic cif files (CCDC numbers 2009243 and 1843016 for compounds 1 and 2, respectively) are available at www.ccdc.cam.ac.uk/data.

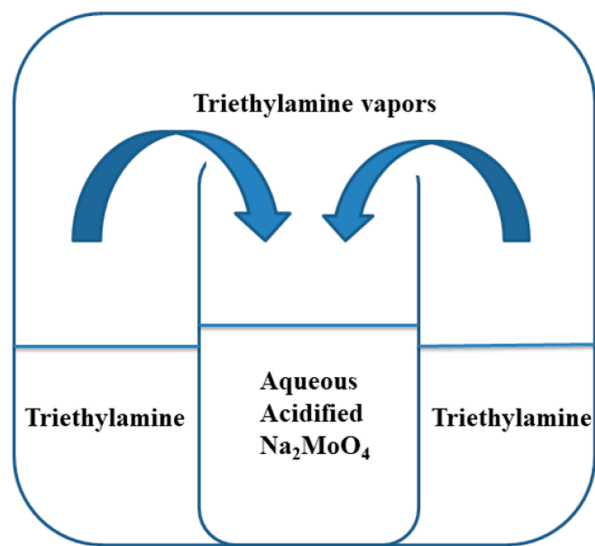
RESULTS AND DISCUSSIONS

Synthesis: Emergence of a Rearrangement Reaction.

When we allowed the triethylamine vapors to diffuse slowly into an acidified aqueous solution of sodium molybdate (Scheme 1), it led to the formation of single crystals of $[(C_2H_5)_3NH]_2[(C_2H_5)_4N][NaMo_8O_{26}]$ (1). Compound 1, as established from single crystal X-ray crystallography, includes the triethylammonium cation, $[(C_2H_5)_3NH]^+$, as expected and, surprisingly, a tetraethylammonium cation $[(C_2H_5)_4N]^+$, even though we have not used any tetraethylammonium salt in the concerned synthesis. To learn the source of the $[(C_2H_5)_4N]^+$ cation, in the crystals of compound $[(C_2H_5)_3NH]_2[(C_2H_5)_4N][NaMo_8O_{26}]$ (1), we carefully investigated the whole experiment and relevant possible chemical reactions; we found out that if the tetraethylammonium cation $[(C_2H_5)_4N]^+$ is formed from triethylamine, $(C_2H_5)_3N$, then the ammonium ion (NH_4^+) has to be generated under an acidic condition as shown in eq 1.

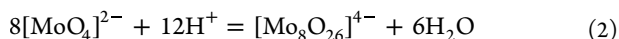
The presence of the ammonium ion in the concerned reaction mixture is confirmed using Nessler's reagent test (*vide infra*) and also by trapping the resulting ammonium ion with

Scheme 1. Schematic Representation of the Experimental Setup for the Synthesis of Compound 1 in a Gas–Liquid Interface Reaction



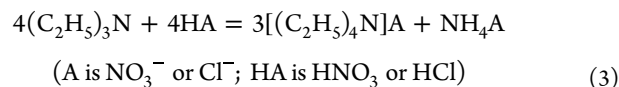
crown ether, forming a supramolecular adduct cation, which is stabilized and isolated with a polyoxometalate (POM) anion (vide infra).

As mentioned above, the diffusion of triethylamine vapors into the acidified solution of sodium molybdate gives compound **1**. In the relevant reaction, we have used HNO₃ and HCl separately in two different experiments, to acidify the solution of sodium molybdate and set the pH of the reaction mixture to 2.0–2.2 (Scheme 1). The presence of the octamolydate isopolyanion, [Mo₈O₂₆]⁴⁻, in compound **1** can be understood by the following reaction (eq 2) of protonation of molybdate anions followed by their condensation leading to the formation of the octamolybdate POM anion.



The coordination of this POM cluster anion with a sodium cation (Na⁺), readily available in the reaction mixture, results in the formation of the [NaMo₈O₂₆]³⁻ anion. This needs three more cations to be isolated. This POM solution was exposed to triethylamine vapor, which, upon its diffusion to the

acidified solution, gets protonated at the vapor–liquid interface, forming the [(C₂H₅)₃NH]⁺ cation. We would not be surprised if the isolated compound **1** would have three [(C₂H₅)₃NH]⁺ cations and have the formula [(C₂H₅)₃NH]₃[NaMo₈O₂₆] (hypothetical); instead, compound **1** is practically characterized with two [(C₂H₅)₃NH]⁺ cations and one “unexpected” tertiary ammonium cation [(C₂H₅)₄N]⁺ with the overall formula [(C₂H₅)₃NH]₂[(C₂H₅)₄N][NaMo₈O₂₆] (**1**). The experiment clearly indicates that the tetraethylammonium cation, [(C₂H₅)₄N]⁺, has been generated from the triethylamine, (C₂H₅)₃N, which is only possible if we consider the following reaction:



Essentially eq 1 and eq 3 are identical.

Notably, one ammonium ion, NH₄⁺, is generated in this reaction (eq 3), which is not included in the crystals of compound [(C₂H₅)₃NH]₂[(C₂H₅)₄N][NaMo₈O₂₆] (**1**). To validate the above-described reaction (eq 1 or 3), thereby, to authenticate the crystal structure of compound **1** (or to prove the formation of the tetraethylammonium cation from triethylamine), we need to prove the existence of the ammonium cation, NH₄⁺ (which is not picked up by compound **1** during its crystal formation) in the pertinent reaction mixture. The most classical and confirmative test for an ammonium ion (NH₄⁺) in an aqueous solution is Nessler’s reagent test, as described below for the NH₄⁺ formed in the rearrangement reaction (eq 1 or 3).

The Nessler’s reagent test was performed on different solutions to detect the presence of ammonium ions in the reaction mixture. First, as a reference, the reagent was added to an ammonium chloride aqueous solution, and as expected, a brown precipitate of HgO·Hg(NH₂)I was observed as shown in Figure 1a. Then the filtrate, obtained after filtering the compound [(C₂H₅)₃NH]₂[(C₂H₅)₄N][NaMo₈O₂₆] (**1**) crystals from the reaction mixture (when the acid used was nitric acid), was treated with a few drops of Nessler’s reagent, and a yellow coloration was observed in the test tube as shown in Figure 1b; similarly, the test was performed also with the filtrate, where HCl acid was used in the place of HNO₃, and there was also a yellow coloration observed (Figure 1c), as in the case of the HNO₃ acid–molybdate reaction mixture. This

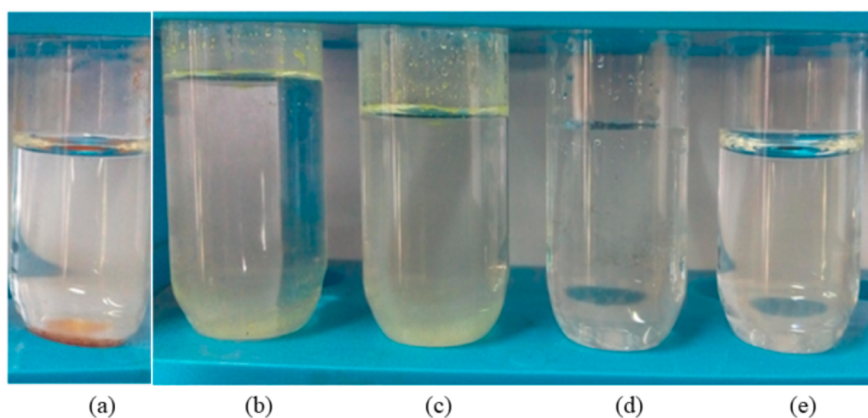
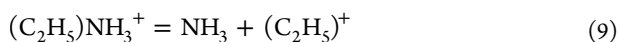
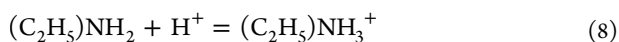
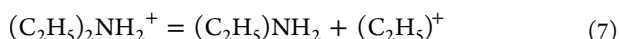
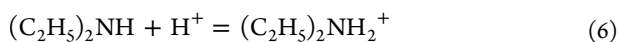
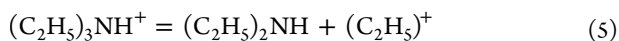
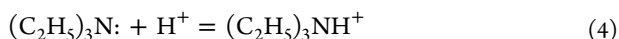


Figure 1. Nessler’s reagent test: (a) with ammonium chloride solution, (b) with filtrate containing HNO₃ acid, (c) with filtrate containing HCl acid, (d) with filtrate containing HNO₃ acid but without sodium molybdate, and (e) with solely water.

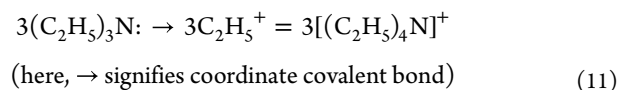
yellow coloration instead of a brown precipitate (found in the case of Nessler's reagent test with NH_4Cl solution) is a result of the brown coloration being affected by dilution. This is because, in the case of diffusion of triethylamine vapor into the acidified sodium molybdate solution, a tiny amount of ammonium ions is formed.

The formation of compound **1** and ammonium ion (eq 3), irrespective of which acid (HNO_3 and HCl acids) has been used, rules out the possibility of the formation of ammonium ions from nitrate ions, which again is a reaction that occurs in drastic conditions.⁴⁷ To check the role of sodium molybdate in the reaction, a controlled reaction was performed, at similar conditions with HNO_3/HCl , but sodium molybdate was not added into it; the resulting reaction yielded no crystals as expected, and also there was no coloration or precipitate observed upon addition of Nessler's reagent to the concerned reaction mixture (Figure 1d). Nessler's reagent was also added to pure water, to check the purity of the reagent, and no change was observed, as can be seen in Figure 1e. Thus, sodium molybdate plays a major role in the formation of the tetraethylammonium ion and in turn the ammonium ion (eq 1 and eq 3).

A careful investigation of eq 1 or eq 3, showing the formation of one equivalent of the ammonium cation (NH_4^+) and three equivalents of tetraethylammonium ($(\text{C}_2\text{H}_5)_4\text{N}^+$) cations from four equivalents of triethylamine ($(\text{C}_2\text{H}_5)_3\text{N}$) under acidic conditions, clearly indicates that one molecule of $(\text{C}_2\text{H}_5)_3\text{N}$ gets into stepwise protonation and subsequent elimination of (C_2H_5) cations until all the ethyl moieties are substituted by protons, yielding the ammonium cation (NH_4^+), as shown in eq 4 – eq 10.



Then the rest three triethylamine molecules $\{3(\text{C}_2\text{H}_5)_3\text{N}\}$, each having a lone pair of electrons on nitrogen, coordinate to the three ethyl cations ($3\text{C}_2\text{H}_5^+$) formed in eq 5, eq 7, and eq 9, resulting in three tetraethylammonium cations, $3[(\text{C}_2\text{H}_5)_4\text{N}]^+$ as shown in eq 11 that shows the formation of three N–C bonds. This equation simply shows the stoichiometry and is not meant to imply accumulation of the indicated species.



The overall reaction of formation of one ammonium ion and three tetraethylammonium cations from four triethylamine molecules and four protons (eq 1 or eq 3) is the result of the formation of four N–H bonds (the number of N–C bonds that break is equal to the number of N–C bonds that form).

This is why eq 1 or eq 3 is probably thermodynamically feasible.

A very important and interesting question now arises regarding the breaking of the stable N–C bond. Here, as we see, the polyoxometalate anion $\{\text{Mo}_8\text{O}_{26}\}^{4-}$ is first formed in the reaction medium, into which the trimethylamine vapors are subjected to diffusion. Here, the polyoxometalate anion plays the role of a catalyst and catalyzes the breaking of the N–C bond. There have been reports where polyoxometalates, viz., $\text{K}_7\text{NiV}_{13}\text{O}_{38} \cdot 16\text{H}_2\text{O}$ ⁴⁸ and $\text{H}_6\text{PMo}_9\text{V}_3\text{O}_{40}$ ⁴⁹ have been used as catalysts for N–C and N=C bond cleavage, respectively. Although the exact mechanism of the catalytic reactions is not clear, still the reactions do not yield the desired product in the absence of the said catalysts. In a very similar way, we could infer from our reaction discussed here that the polyoxometalate anion plays the role of the catalyst for the N–C bond cleavage shown in eq 5, eq 7, and eq 9.

Serendipitous Observation in Crystal Structure Analysis. A gas–liquid interface reaction via diffusion of volatile amine vapors into an acidified molybdate aqueous solution to generate a polyoxometalate (POM) cluster is a very simple synthetic approach to obtain a POM cluster containing compound, and we developed this approach recently.⁵⁰

Thus, diffusion of pyridine (py) and piperidine (pip) into an acidified aqueous solution of sodium molybdate results in the isolation of single crystals of pyridinium and piperidinium salts of octamolybdate, $[\text{pyH}]_4[\text{Mo}_8\text{O}_{26}]$, and $[\text{pipH}]_4[\text{Mo}_8\text{O}_{26}] \cdot 4\text{H}_2\text{O}$, respectively. This synthetic strategy has been described as a potential bag filter for volatile organic amines. This has an important implication in the sense that volatile amine vapors are serious threats to human health.⁴⁸ We wanted to rationalize this concept by studying another volatile amine, and we used triethylamine vapors, in the present work, to diffuse into an acidified aqueous solution of Na_2MoO_4 ; we obtained the single crystals of compound $[(\text{C}_2\text{H}_5)_3\text{NH}]_2[(\text{C}_2\text{H}_5)_4\text{N}][\text{NaMo}_8\text{O}_{26}]$ (**1**). We have made a serendipitous observation while analyzing the single crystal X-ray structure of compound **1**. We found a tetraethylammonium cation $[(\text{C}_2\text{H}_5)_4\text{N}]^+$ per formula unit of compound **1** in its crystal structure, even though we have not used any tetraethylammonium salt in the pertinent synthesis. The crystal structure analysis of compound **1** is described below.

Compound **1** crystallizes in a monoclinic $C2/c$ space group. The asymmetric unit of the compound consists of half of an octamolybdate cluster, i.e., a $\{\text{Mo}_4\text{O}_{13}\}^{2-}$ unit, in which the surface oxygens are coordinated to a Na^+ cation with half occupancy, forming a $\{\text{Na}_{0.5}\text{Mo}_4\text{O}_{13}\}^{1.5-}$ unit, a protonated triethylamine cation, and half of a tetraethylammonium cation, as shown in Figure 2a. Accordingly, in the full molecule, two halves of the two different clusters coordinating to a common sodium ion, a tetraethylammonium cation, and two protonated triethylamine cations are present as shown in Figure 2b. Thus, in the crystal structure of compound **1**, an octamolybdate cluster anion coordinates to two Na^+ ions from its opposite sides (on each side, four surface terminal oxygen atoms of the cluster coordinate to the sodium ion), resulting in the formation of a chainlike one-dimensional coordination polymer. Along the chain, each sodium ion is eight coordinated, and the sodium ions are arranged in a zigzag fashion throughout the molecular structure (Figure S2, SI). The relevant $\text{Na}^+\text{--O}$ bond distances are in the range of 2.545–2.666 Å.

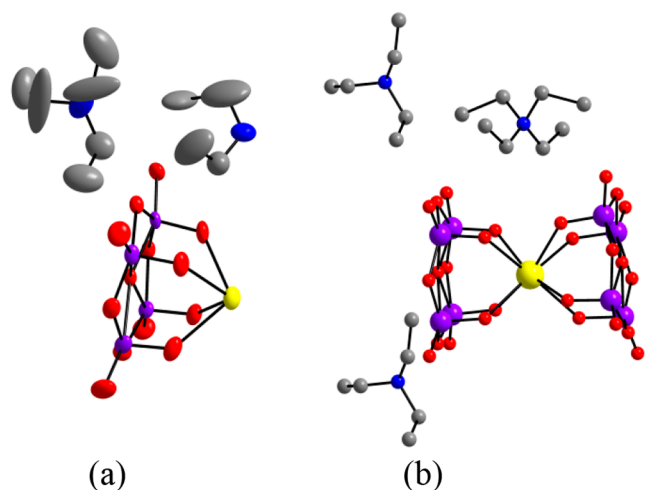


Figure 2. (a) Thermal ellipsoidal diagram of the asymmetric unit in the crystal structure of compound **1** at the 50% probability level. (b) Full molecule of compound **1** showing that two different halves of two different $[\text{Mo}_8\text{O}_{26}]^{4-}$ clusters are coordinated to a central Na^+ ion. Hydrogen atoms are not shown for clarity. Color code: Mo, purple; Na, yellow; O, red; N, blue; C, gray.

The tetraethylammonium cation and some of the cluster oxygen atoms are hydrogen bonded to each other, leading to a 3D supramolecular network in the crystal structure of compound **1**. The serendipitous observation of a tetraethylammonium cation, $[(\text{C}_2\text{H}_5)_4\text{N}]^+$, in the crystals of compound **1** gives rise to the emergence of a new rearrangement reaction (eq 1), as already mentioned earlier.

It is not surprising that the ammonium ion, produced in the rearrangement (eq 1 or eq 3), is not included in the crystals of compound **1**, because the cations $[(\text{C}_2\text{H}_5)_3\text{NH}]^+$ and $[(\text{C}_2\text{H}_5)_4\text{N}]^+$, present in the concerned reaction mixture with the NH_4^+ ion, are bulkier than the NH_4^+ ion. However, the ammonium ion in the mother liquor of compound **1** crystals can be associated with the crown ether, benzo-15-crown-5 (B15C5), when the mother liquor of compound **1** crystals is treated with B15C5 crown ether and a Keggin type polyoxometalate (POM) anion. More specifically, the $[\text{NH}_4^+\text{CB15C5}]$ supramolecular cationic species forms a cation–anion adduct with the $[\text{PMo}_{12}\text{O}_{40}]^{3-}$ Keggin anion in an acidified organic medium leading to the isolation of single crystals of compound $[\text{NH}_4\text{CB15C5}]_3[\text{PMo}_{12}\text{O}_{40}]\cdot\text{B15C5}$ (**2**). The asymmetric unit in the crystal structure of compound **2**, which crystallizes in the $P\bar{1}$ space group (triclinic, $Z' = 1$), consists of two halves of the $[\text{PMo}_{12}\text{O}_{40}]^{3-}$ Keggin anion, three ammonium ions associated benzo-15-crown-5 crown ether supramolecular cations, and one benzo-15-crown-5 without any ammonium ion. Thus, the asymmetric unit represents the full molecular formula of compound $[\text{NH}_4\text{CB15C5}]_3[\text{PMo}_{12}\text{O}_{40}]\cdot\text{B15C5}$ (**2**) in this case (Figure 3). All three ammonium ions (N1, N3, and N4 nitrogen atoms in the crystal structure, shown in Figure 4) are not located in the cavities of the crown ethers and have different hydrogen bonding environments. The N4 ammonium ion interacts with the Keggin POM anion (terminal oxygen atom) in addition to its hydrogen bonding interactions with the crown ether molecule. On the other hand, the N1 and N3 ammonium ions, in addition to their interactions with two different crown ether molecules, are hydrogen bonded to a common crown ether molecule as shown in Figure 4. Thus, we could characterize the NH_4^+ ion,

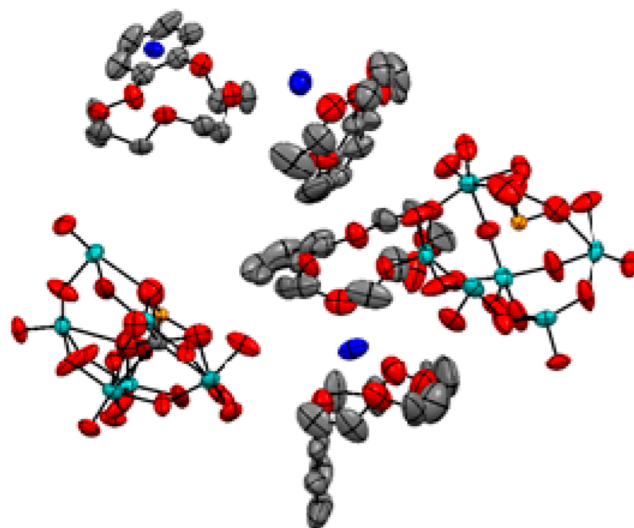


Figure 3. Thermal ellipsoidal diagram of the asymmetric unit in the crystal structure of compound **2** at the 50% probability level, representing the full molecule. Hydrogen atoms are omitted for clarity. Color code: Mo, cyan; O, red; C, gray; P, orange; N, blue.

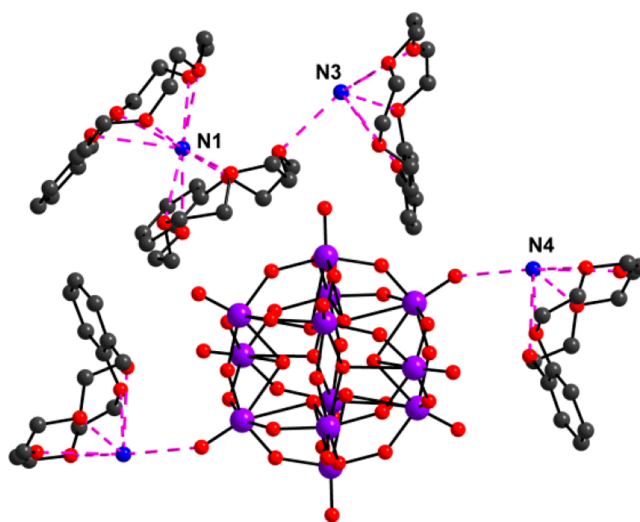


Figure 4. Hydrogen bonding interactions around ammonium ions in the crystal structure of compound $[\text{NH}_4\text{CB15C5}]_3[\text{PMo}_{12}\text{O}_{40}]\cdot\text{B15C5}$ (**2**). Purple dotted lines represent N–H...O hydrogen bonding interactions.

formed in the rearrangement reaction (eq 1 or eq 3), crystallographically in the crystals of compound $[\text{NH}_4\text{CB15C5}]_3[\text{PMo}_{12}\text{O}_{40}]\cdot\text{B15C5}$ (**2**). It is surprising that crystals include the NH_4^+ cation instead of $[(\text{C}_2\text{H}_5)_3\text{NH}]^+$ and $[(\text{C}_2\text{H}_5)_4\text{N}]^+$ cations, which are also present with the NH_4^+ ion in the concerned filtrate of compound **1** crystals. This can be understood by the fact that the NH_4^+ cation–crown ether association seems to be much stronger than the $[(\text{C}_2\text{H}_5)_3\text{NH}]^+$ – and $[(\text{C}_2\text{H}_5)_4\text{N}]^+$ –crown ether associations because of the formation of N–H...O hydrogen bonds (NH_4^+ can form four H-bonds, $[(\text{C}_2\text{H}_5)_3\text{NH}]^+$ can form only one H-bond, and $[(\text{C}_2\text{H}_5)_4\text{N}]^+$ cannot form any N–H...O bond). The rearrangement reaction (eq 1 or 3) is characterized not only by Nessler's reagent test and single crystal X-ray crystallography (vide supra) but also by IR, ^1H NMR, and ESI-mass

spectral studies including TGA analysis as described in the following sections.

Spectroscopy. IR Spectroscopy. The Fourier transform infrared (FTIR) spectrum of compound **1** was recorded and is shown in Figure S5a,b in the SI. The vibrational features of the octamolybdate isopolyanion are clearly seen in the IR spectrum of the compound (Figure S5b). The strong peak at 955 cm^{-1} can be attributed to the asymmetric stretch of the Mo–O_t bond. Similarly, the asymmetric stretch of the Mo–O_b–Mo bond is found at 730 cm^{-1} . The peaks at 730, 780, 838, and 898 cm^{-1} are the characteristic peaks for the Mo–O_b asymmetric stretch. All these values almost match the vibrational features reported for the β -isomer of the octamolybdate in the literature.^{51,52} The strong peak at 1214 cm^{-1} can be attributed to the C–N stretch. The peaks at 1380 and 1470 cm^{-1} can be attributed to CH₂ and CH₃ bending of the ethyl groups, and the peaks at 2872 and 2968 cm^{-1} can be attributed to the C–H stretch. In the FTIR spectrum of compound **2** (Figure S5c,d), the peak at 3182 cm^{-1} can be attributed to the stretching frequency of the N–H bonds of the ammonium ions. Similarly, the bending motions of the N–H bonds give their signature peaks at 1356 cm^{-1} . The peak at 2916 cm^{-1} is actually a multiplet centered on this point. These peaks can be attributed to the alkyl C–H stretch, which is present in the crown ethers. The various peaks around 778, 892, 978, 1053, and 1077 cm^{-1} can be attributed to the stretching frequencies of Mo–O_c–Mo, Mo–O_b–Mo, Mo=O_v, and the P–O bonds, respectively, of the Keggin cluster anion (Figure S5d).⁵³

¹H NMR Spectroscopy. ¹H NMR spectrum of compound [NH₄CB15CS]₃[PMo₁₂O₄₀]·B15CS (**2**) has been recorded in DMSO-*d*₆ at room temperature and is given in Figure 5.

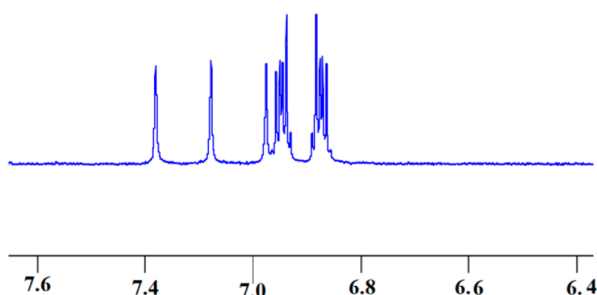


Figure 5. ¹H NMR spectrum of the compound [NH₄CB15CS]₃[PMo₁₂O₄₀]·B15CS (**2**), showing shifts and splitting of the NH₄⁺ signals.

NH₄Cl shows a strong singlet at $\delta\ 7.49$ in DMSO-*d*₆,⁵⁴ although, because of the coupling of ¹H to the ¹⁴N quadrupolar nucleus, it should give a triplet of equal intensity.⁵⁵ But, in practice, because of the tetrahedral structure of the NH₄⁺ cation, we see only a narrow line for ¹⁴NH₄⁺. In the case of compound [NH₄CB15CS]₃[PMo₁₂O₄₀]·B15CS (**2**), because of the hydrogen bonding interactions of the ammonium cations with the crown ether as well as with the polyoxometalate anion, NH₄⁺ does not retain its tetrahedral structure, and hence, by virtue of quadrupolar coupling, it shows triplets of equal intensity between $\delta\ 6.97$ and 7.35 as shown in Figure 5. The credible cause for this upfield shifting of the signals might be due to a shielded environment around the ion interacting with lone pair on O atoms of crown ether. The full ¹H NMR spectra of compound **2**, NH₄Cl, and B15CS

crown ether in DMSO-*d*₆ are provided with the SI as Figures S6, S7, and S8, respectively.

ESI-MS. The ESI-MS spectra of the compound [NH₄CB15CS]₃[PMo₁₂O₄₀]·B15CS (**2**) were also studied to confirm the presence of the ammonium cations in compound **2**. Among various other peaks, the base peak having the *m/z* value of 554.2880 can be attributed to the molecular fragment having two {benzo-15-crown-5} moieties and one ammonium cation (Figure S9, SI), thus confirming the presence of the ammonium cations in the compound.

Thermogravimetric Analysis. The thermal stabilities of both compound **1** and compound **2** were evaluated using thermogravimetric analysis, and the relevant plots are shown in Figure S10 (SI). In compound **1**, the organic cations, viz., the two protonated triethylamine and the tetraethylamine are decomposed in the temperature range of $100\text{ }^{\circ}\text{C}$ to around $370\text{ }^{\circ}\text{C}$, followed by the breaking up of the Na⁺–octamolybdate 1-D chain, hence, leaving the metal oxides (sodium oxide and molybdenum oxide) in the higher temperature range. The thermal stability of compound **2** was also checked and is represented in Figure S10b (SI). The ammonium ions that are arrested by the crown ether moieties are liberated first upon heating up to almost $150\text{ }^{\circ}\text{C}$, followed by the crown ether molecules in the temperature range of $280\text{--}580\text{ }^{\circ}\text{C}$. Then the Keggin polyoxometalate anion remains in the crucible and is stable up to $700\text{ }^{\circ}\text{C}$. After this temperature, the Keggin cluster starts decomposing.

The major finding of this work is that we have established a unique rearrangement reaction (eq 1 or eq 3) producing ammonium ions at room temperature from triethylamine in an acidic aqueous polyoxometalate solution. Thus, the present system, where no ammonia has been used but triethylamine is diffused, shows the formation of the ammonium ion, which has been established not only by elemental analyses (Figure S13, SI), Nessler's reagent test, thermal analysis, and EDAX analysis (Figure S14, Table S1, SI) but also by NMR spectroscopy and single crystal X-ray crystallography, including ESI–mass spectroscopy.

CONCLUSION

With this work on a polyoxometalate system to yield the NH₄⁺ ion at room temperature, we have made an attempt to establish a hitherto unknown rearrangement reaction, $4(\text{C}_2\text{H}_5)_3\text{N} + 4\text{H}^+ \rightarrow 3[(\text{C}_2\text{H}_5)_4\text{N}]^+ + [\text{NH}_4]^+$ (eq 1), which generates an ammonium ion at room temperature from triethylamine simply by diffusion of the latter into an acidified aqueous solution of sodium molybdate. The *in situ* formed polyoxometalate plays a vital role in the generation of ammonium ions, which is serendipitous in nature. Although we could not establish yet the quantity of ammonia generated in this reaction because of the uncontrolled vapor–liquid interface reaction, still it provides a unique rearrangement reaction for the generation of ammonia from triethylamine at ambient conditions.

ASSOCIATED CONTENT

Supporting Information

The Supporting Information is available free of charge at <https://pubs.acs.org/doi/10.1021/acsomega.2c04015>.

Figures S1–S14 (crystal structures, FT-IR and ¹H NMR spectra, ESI-MS, TGA, and PXRD plots); Tables S1, S2,

S3, and S4 (crystal parameters, EDAX table, and bond lengths and bond angles of compounds 1 and 2) (PDF)
X-ray crystallographic data for compound 1 (CIF)
X-ray crystallographic data for compound 2 (CIF)

AUTHOR INFORMATION

Corresponding Author

Samar K. Das – School of Chemistry, University of Hyderabad, Hyderabad, Telangana 500046, India;
orcid.org/0000-0002-9536-6579; Phone: +91 40 2313 4853; Email: skdas@uohyd.ac.in, samar439@gmail.com

Authors

N. Tanmaya Kumar – School of Chemistry, University of Hyderabad, Hyderabad, Telangana 500046, India
Shivaiah Vaddypally – Department of Chemistry, Temple University, Philadelphia, Pennsylvania 19122, United States;
orcid.org/0000-0001-6203-9689

Complete contact information is available at:

<https://pubs.acs.org/10.1021/acsomega.2c04015>

Author Contributions

The manuscript was written through contributions of all authors. All authors have given approval to the final version of the manuscript.

Funding

IoE, University of Hyderabad (Project No. RC1–20–007) and DST-SERB, Government of India (Project No. EMR/2017/002971).

Notes

The authors declare no competing financial interest.

ACKNOWLEDGMENTS

The project is supported by DST-SERB (Project No. EMR/2017/002971), the UGC-BSR Project (Project No. 19-232/2019(BSR)), and the IoE, University of Hyderabad (Project No. RC1-20-007). We also acknowledge DST-FIST, UGC-SAP, and UPE-II for facilities. N.T.K. thanks CSIR, India, for a fellowship. The authors thank Dr. K. Sathish for his valuable suggestions in crystallography.

REFERENCES

- (1) Modak, J. M. Haber process for ammonia synthesis. *Resonance* **2002**, *7*, 69.
- (2) Schrock, R. R. Catalytic reduction of dinitrogen to ammonia at a single molybdenum center. *Acc. Chem. Res.* **2005**, *38*, 955–962.
- (3) Schrock, R. R. Reduction of dinitrogen. *Proc. Natl. Acad. Sci. U.S.A.* **2006**, *103*, 17087–17087.
- (4) Howard, J. B.; Rees, D. C. How many metals does it take to fix N₂? A mechanistic overview of biological nitrogen fixation. *Proc. Natl. Acad. Sci. U.S.A.* **2006**, *103*, 17088–17093.
- (5) Green, L., Jr. An ammonia energy vector for the hydrogen economy. *Int. J. Hydrogen Energy* **1982**, *7*, 355–359.
- (6) Lan, R.; Irvine, J. T. S.; Tao, S. Ammonia and related chemicals as potential indirect hydrogen storage materials. *Int. J. Hydrogen Energy* **2012**, *37*, 1482–1494.
- (7) Fenwick, A. Q.; Gregoire, J. M.; Luca, O. R. Electrocatalytic reduction of nitrogen and carbon dioxide to chemical fuels: challenges and opportunities for a solar fuel device. *J. Photochem. Photobiol., B* **2015**, *152*, 47–57.
- (8) Aika, K.; Christiansen, L. J.; Dybkjaer, I.; Hansen, J. B.; Nielsen, A.; Stoltze, P.; Tamaru, K.; *Ammonia*; Springer: Germany, 1995.
- (9) Schlogl, R. Catalytic synthesis of ammonia- a “never ending story”? *Angew. Chem., Int. Ed.* **2003**, *42*, 2004–2008.
- (10) Ertl, G. Reactions at surfaces: from atoms to complexity. *Angew. Chem., Int. Ed.* **2008**, *47*, 3524–3535.
- (11) Rees, D. C.; Howard, J. B. Nitrogenase: standing at the crossroads. *Curr. Opin. Chem. Biol.* **2000**, *4*, 559–566 (and references therein).
- (12) Burgess, B. K. The iron-molybdenum cofactor of nitrogenase. *Chem. Rev.* **1990**, *90*, 1377–1406.
- (13) Burgess, B. K.; Lowe, D. J. Mechanism of molybdenum nitrogenase. *Chem. Rev.* **1996**, *96*, 2983–3011.
- (14) Ashida, Y.; Arashiba, K.; Nakajima, K.; Nishibayashi, Y. Molybdenum-catalysed ammonia production with samarium diiodide and alcohols or water. *Nature* **2019**, *568*, 536–540.
- (15) Yandulov, D. V.; Schrock, R. R. Catalytic reduction of dinitrogen to ammonia at a single molybdenum center. *Science* **2003**, *301*, 76–78.
- (16) Nishibayashi, Y. *Nitrogen fixation*, 1st ed.; Topics in organometallic chemistry; Springer: Heidelberg, 2017; Vol. 60.
- (17) Arashiba, K.; Miyake, Y.; Nishibayashi, Y. A molybdenum complex bearing PNP-type pincer ligands leads to the catalytic reduction of dinitrogen into ammonia. *Nat. Chem.* **2011**, *3*, 120–125.
- (18) Anderson, J. S.; Rittle, J.; Peters, J. C. Catalytic conversion of nitrogen to ammonia by an iron model complex. *Nature* **2013**, *501*, 84–87.
- (19) Fajardo, J., Jr.; Peters, J. C. Catalytic nitrogen-to-ammonia conversion by osmium and ruthenium complexes. *J. Am. Chem. Soc.* **2017**, *139*, 16105–16108.
- (20) Arashiba, K.; Eizawa, A.; Tanaka, H.; Nakajima, K.; Yoshizawa, K.; Nishibayashi, Y. Catalytic nitrogen fixation via direct cleavage of nitrogen-nitrogen triple bond of molecular dinitrogen under ambient reaction conditions. *Bull. Chem. Soc. Jpn.* **2017**, *90*, 1111–1118.
- (21) Chatt, J.; Pearman, A. J.; Richards, R. L. The reduction of mono-coordinated molecular nitrogen to ammonia in a protic environment. *Nature* **1975**, *253*, 39–40.
- (22) Li, H.; Shang, J.; Ai, Z.; Zhang, L. Efficient visible light nitrogen fixation with BiOBr nanosheets of oxygen vacancies on the exposed {001} facets. *J. Am. Chem. Soc.* **2015**, *137*, 6393–6399.
- (23) Hirakawa, H.; Hashimoto, M.; Shiraishi, Y.; Hirai, T. Photocatalytic conversion of nitrogen to ammonia with water on surface oxygen vacancies of titanium dioxide. *J. Am. Chem. Soc.* **2017**, *139*, 10929–10936.
- (24) Brown, K. A.; Harris, D. F.; Wilker, M. B.; Rasmussen, A.; Khadka, N.; Hamby, H.; Keable, S.; Dukovic, G.; Peters, J. W.; Seefeldt, L. C.; King, P. W. Light-driven dinitrogen reduction catalyzed by a CdS: nitrogenase MoFe protein biohybrid. *Science* **2016**, *352*, 448–450.
- (25) Guha, A.; Narayanaru, S.; Kaley, N. M.; Rao, D. K.; Mondal, J.; Narayanan, T. N. Mechanistic insight into high yield electrochemical nitrogen reduction to ammonia using lithium ions. *Mater. Today Comm.* **2019**, *21*, 100700.
- (26) Lan, R.; Irvine, J. T. S.; Tao, S. Synthesis of ammonia directly from air and water at ambient temperature and pressure. *Sci. Rep.* **2013**, *3*, 1145.
- (27) Cui, B.; Zhang, J.; Liu, S.; Xiang, W.; Liu, L.; Xin, H.; Lefler, M. J.; Licht, S.; Liu, X. Electrochemical synthesis of ammonia directly from N₂ and water over iron-based catalysts supported on activated carbon. *Green Chem.* **2017**, *19*, 298–304.
- (28) Manjunatha, R.; Karajic, A.; Goldstein, V.; Schechter, A. Electrochemical ammonia generation directly from nitrogen and air using an iron-oxide/titania-based catalyst at ambient conditions. *ACS Appl. Mater. Interfaces* **2019**, *11* (8), 7981–7989.
- (29) Cong, L.; Yu, Z.; Liu, F.; Huang, W. Electrochemical synthesis of ammonia from N₂ and H₂O using a typical non-noble metal carbon-based catalyst under ambient conditions. *Catal. Sci. Technol.* **2019**, *9*, 1208–1214.
- (30) Giddey, S.; Badwal, S. P. S.; Kulkarni, A. Review of electrochemical ammonia production technologies and materials. *Int. J. Hydrog. Energy* **2013**, *38*, 14576–14594.

- (31) Licht, S.; Cui, B.; Wang, B.; Li, F.-F.; Lau, J.; Liu, S. Ammonia synthesis by N₂ and steam electrolysis in molten hydroxide suspension of nanoscale Fe₂O₃. *Science* **2014**, *345*, 637–640.
- (32) Kyriakou, V.; Garagounis, I.; Vasileiou, E.; Vourros, A.; Stoukides, M. Progress in the electrochemical synthesis of ammonia. *Catal. Today* **2017**, *286*, 2–13.
- (33) Bao, D.; Zhang, Q.; Meng, F. L.; Zhong, H.; Shi, M.-M.; Zhang, Y.; Yan, J.-M.; Jiang, Q.; Zhang, X.-B. Electrochemical reduction of N₂ under ambient conditions for artificial N₂ fixation and renewable energy storage using N₂/NH₃ cycle. *Adv. Mater.* **2017**, *29*, 1604799.
- (34) Oshikiri, T.; Ueno, K.; Misawa, H. Selective dinitrogen conversion to ammonia using water and visible light through plasmon-induced charge separation. *Angew. Chem. Int. ed.* **2016**, *55*, 3942–3946.
- (35) Zheng, J.; Lyu, Y.; Qiao, M.; Wang, R.; Zhou, Y.; Li, H.; Chen, C.; Li, Y.; Zhou, H.; Jiang, S. P.; Wang, S. Photoelectrochemical synthesis of ammonia on the aerophilic-hydrophilic heterostructure with 37.8% efficiency. *Chem.* **2019**, *5*, 617–633.
- (36) Ali, M.; Zhou, F.; Chen, K.; Kotzur, C.; Xiao, C.; Bourgeois, L.; Zhang, X.; MacFarlane, D. R. Nanostructured photoelectrochemical solar cell for nitrogen reduction using plasmon-enhanced black silicon. *Nat. Commun.* **2016**, *7*, 11335.
- (37) Oshikiri, T.; Ueno, K.; Misawa, H. Ammonia photosynthesis via an association pathway using a plasmonic photoanode and a zirconium cathode. *Green Chem.* **2019**, *21*, 4443–4448.
- (38) Guo, C.; Ran, J.; Vasileff, A.; Qiao, S.-Z. Rational design of electrocatalyst and photo(electro)catalysts for nitrogen reduction to ammonia (NH₃) under ambient conditions. *Energy Environ. Sci.* **2018**, *11*, 45–56.
- (39) Bhattacharya, A. K.; Thyagarajan, G. The Michaelis-Arbuzov Rearrangement. *Chem. Rev.* **1981**, *81*, 415–430.
- (40) Muetterties, E. L.; Hoel, E. L.; Salentine, C. G.; Hawthorne, M. F. Intermolecular rearrangements in boron clusters. *Inorg. Chem.* **1975**, *14*, 950–951.
- (41) Satapathi, S. In situ rearrangement of polyamines in the presence of different metal ions. *Inorg. Chem. Commun.* **2015**, *56*, 89–101.
- (42) *Triethylamine*; U.S. EPA: 1993.
- (43) *Bruker SMART*, Version 5.625; *SHELXTL*, Version 6.12; Bruker AXS Inc.: Madison, WI, U.S.A., 2000.
- (44) Sheldrick, G. M. *Program for Refinement of Crystal Structures*; University of Göttingen, Germany, 1997.
- (45) Sheldrick, G. M. *Acta Crystallogr., Sect. A: Found. Crystallogr.* **2008**, *64*, 112–122.
- (46) Sheldrick, G. M. Crystal structure refinement with SHELXL. *Acta Crystallogr., Sect. C: Struct. Chem.* **2015**, *71*, 3–8.
- (47) Summers, D. P. Ammonia formation by the reduction of nitrite/nitrate by FeS. *Orig. Life Evol. Biosph.* **2005**, *35*, 299–312.
- (48) Gao, F.; Hua, R. Novel C–N bond cleavage and formation in the polyoxometalates-catalyzed oxidation of nitroaromatics with 30% aqueous H₂O₂: An unprecedented disproportionation of nitroaromatics affording dinitroaromatics. *Inorg. Chim. Acta* **2005**, *358*, 4045–4048.
- (49) Heravi, M. M.; Ranjbar, L.; Derikvand, F.; Oskooie, H. A.; Bamoharram, F. F. Catalytic oxidative cleavage of C–N bond in the presence of mixed-addenda vanadomolybdophosphate, H₆PMo₉V₃O₄₀ as a green and reusable catalyst. *J. Mol. Catal. A: Chem.* **2007**, *265*, 186–188.
- (50) Shivaiah, V.; Kumar, N. T.; Das, S. K. A gas-liquid interface synthesis in polyoxometalate chemistry: potential bag filter for volatile organic amines. *J. Chem. Sci.* **2018**, *130*, 37.
- (51) Rosnes, M. H.; Yvon, C.; Long, D.-L.; Cronin, L. Mapping the synthesis of low nuclearity polyoxometalates from octamolybdates to Mn-Anderson clusters. *Dalton Trans.* **2012**, *41*, 10071–10079.
- (52) Zebiri, I.; Boufas, S.; Mosbah, S.; Bencharif, L.; Bencharif, M. Synthesis and structural characterization of (C₁₄H₁₆N₂)₃(C₁₄H₁₇N₂)₂[β-Mo₈O₂₆]. *J. Chem. Sci.* **2015**, *127*, 1769–1775.
- (53) Aouissi, A.; Al-Othman, Z. A.; Al-Anezi, H. Reactivity of heteropolymolybdates and heteropolytungstates in cationic polymerization of styrene. *Molecules* **2010**, *15*, 3319–3328.
- (54) Chatterjee, T.; Sarma, M.; Das, S. K. Supramolecular architectures from ammonium-crown ether inclusion complexes in polyoxometalate association: synthesis, structure and spectroscopy. *Cryst. Growth Des.* **2010**, *10*, 3149–3163.
- (55) Ebsworth, E. A. V.; Rankin, D. W. H.; Cradock, S. *Structural methods in inorganic chemistry*, 2nd ed.; Blackwell: 1991; pp 51–52.

Recommended by ACS

Iodine-Mediated Furoxan Formation Facilitates the Synthesis of High-Density Tricyclic Fused Energetic Materials

Lei Yang, Jinshan Li, *et al.*

NOVEMBER 29, 2022

CRYSTAL GROWTH & DESIGN

READ 

Synthesis of a Polyoxometalate-Encapsulated Metal–Organic Framework via *In Situ* Ligand Transformation Showing Highly Catalytic Activity in Both Hydrogen Evolution an...

Zhuanfang Zhang, Chunyan Zhao, *et al.*

JULY 19, 2022

INORGANIC CHEMISTRY

READ 

Self-Assembly of a Pd₄Cu₈L₈ Cage for Epoxidation of Styrene and Its Derivatives

Xian-Chao Zhou, Dan Li, *et al.*

MARCH 24, 2022

INORGANIC CHEMISTRY

READ 

Synthesis, Structure, and Heterogeneous Catalysis of a Series of Structurally Diverse Coordination Polymers Based on 5-Nitroisophthalate

Subham Sahoo and Debajit Sarma

AUGUST 08, 2022

CRYSTAL GROWTH & DESIGN

READ 

Get More Suggestions >